Density functional theory of liquid crystals and surface anchoring

M. Moradi*
Department of Physics, College of Science, Shiraz University, Shiraz 71454, Iran

Richard J. Wheatley
School of Chemistry, University of Nottingham, University Park, Nottingham NG7 2RD, United Kingdom

A. Avazpour†
Department of Physics, College of Science, Shiraz University, Shiraz 71454, Iran and Department of Physics, College of Science, Yasooj University, Yasooj 75919, Iran

(Received 5 May 2005; revised manuscript received 21 October 2005; published 23 December 2005)

This paper applies the density functional theory to confined liquid crystals comprising ellipsoidal shaped particles interacting through the hard Gaussian overlap (HGO) potential. The restricted orientation model proposed by Rickayzen [Mol. Phys. **95**, 393 (1998)] is extended to study the surface anchoring. The excess free energy is calculated as a functional expansion of density around a reference homogeneous fluid. The pair direct correlation function (DCF) of a homogeneous HGO fluid is approximated, based on the Percus-Yevick DCF for hard spheres; the anisotropy is introduced by means of the closest approach parameter. The average number density and orientational order parameter profiles of a HGO fluid confined in between planar walls are obtained using a hard needle-wall potential to represent the particle-wall interactions. For short and long needle lengths, the homeotropic and planar anchoring are observed, respectively. For the bulk isotropic phase the calculated density and order parameter profiles are in agreement with the Monte Carlo simulation of Barmes and Cleaver [Phys. Rev. E **69**, 61705 (2004)]. However, for the bulk nematic phase the theory gives the correct density profile between the walls. The correct order parameters are obtained close to the walls whereas for the region in the middle of the walls, the agreement is less satisfactory.

DOI: 10.1103/PhysRevE.72.061706 PACS number(s): 61.30.Cz, 61.20.Gy, 64.70.Md, 68.08.−p

I. INTRODUCTION

The structure of confined liquid crystals plays an important role in the technology of liquid crystal displays [1–3]. When a liquid crystal is placed in contact with another phase, in particular a solid, the surface induces structural changes in the liquid [4,5]. The tendency of liquid crystals to orient in a particular direction when in contact with the container wall is called anchoring [6,7]. This phenomenon of orientation of a liquid crystal is very similar to epitaxy of a solid on a substrate. The effects of surface and anchoring in liquid crystals are reviewed by Jerome [1] and a brief review of the anchoring transition at liquid crystal surfaces is given by Slukin [8]. The concept of anchoring may be assumed as analogous to the concept of the phase for the state of matter. The anchoring induced by an interface is known as planar, tilted, or homeotropic depending on whether the anchoring directions are, respectively, parallel, tilted, or perpendicular to the plane of the interface. The influence of the surface on liquid crystals is an interesting subject from the theoretical and experimental point of view [4,9,10].

In this paper we use a density functional theory to study the surface influence on liquid crystalline systems. Since in the liquid crystal the elastic theory [6] is completely inapplicable when the density, the direction of ordering, and the order parameter vary rapidly with positions [9], the density functional theory is helpful. Density functional theories [11] are capable of predicting the phase diagram of liquid crystals [12,13], including translational ordered phases such as smectics, and of describing the structure near a solid surface. Allen [6] showed that even the simplest density functional theory, the Onsager theory [14], can describe the structure of the surface layer under the influence of an external perturbation. Density functional theory has also been used to study the thermodynamics of homogeneous molecular fluids [15] and structural properties of inhomogeneous molecular fluids, such as hard ellipsoids [16,17], hard circular cylinders [18], and hard Gaussian overlap (HGO) [19] fluids confined between planar walls. Here we use a simple model of liquid crystals, where the interaction potential between the particles is assumed to be of a HGO type [20,21].

We use the hypernetted chain (HNC) density functional proposed by Rickayzen and co-workers [16], and extend their restricted orientation model to study confined HGO fluids comprising molecules which can be aligned in more than six directions. The grand potential as a functional of the number density of molecules is minimized to obtain the number densities, density profiles, and order parameters of a liquid crystal confined between planar walls. We then consider the surface anchoring, study the anchoring transition from planar to homeotropic alignment, and compare our results with Monte Carlo simulations [22]. In this paper we show that for the bulk isotropic density, the density functional theory used here gives the correct results for the density and the order parameter profiles. In addition, we show

*Electronic address: moradi@physics.susc.ac.ir
†Electronic address: avazpour@mail.yu.ac.ir

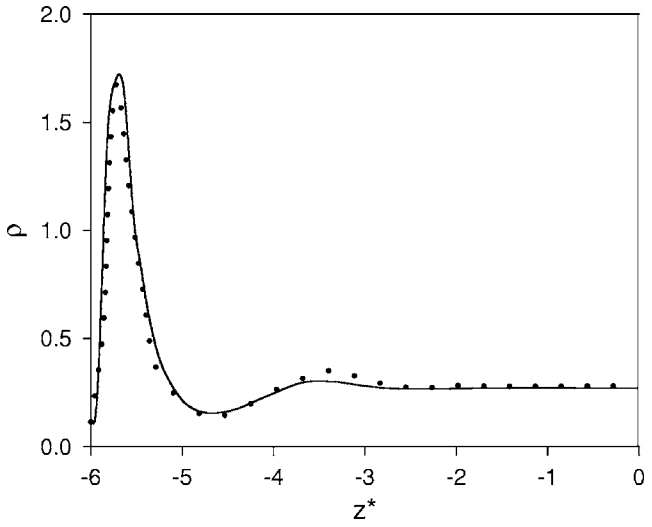

FIG. 1. Number density profiles of molecules as a function of reduced distance from the center of slit, z^*, for $k=3$, $\rho_B=0.246$, $k_s=0.6$, and $h^*=12$. The solid curve is our calculation and the dots are from the Monte Carlo simulation [22].

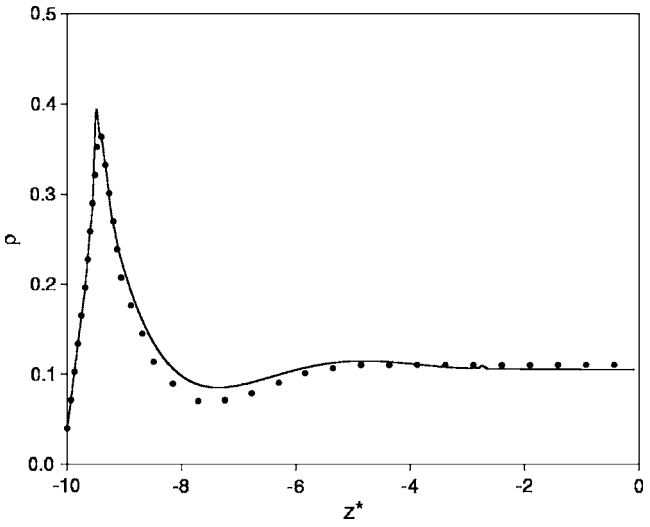

FIG. 3. Number density profiles of molecules as a function of z^* for $k=5$, $k_s=1$, $\rho_B=0.1$, and $h^*=20$. The solid curve is our calculation and the dots are from the Monte Carlo simulation [29].

that for the nematic bulk density the correct angular averaged density profile can be obtained anywhere between the walls, whereas the correct order parameter can be obtained near the walls and there are some discrepancies in the middle of the walls. In Sec. II we describe the density functional theory of molecular fluids confined between planar walls, and in Sec. III we obtain the direct correlation function of HGO fluids. Finally, in Sec. IV we obtain the results and present our conclusions.

II. THEORY

We consider the grand potential of a molecular fluid confined in between parallel planar walls as a functional of number density ρ, and we choose the z axis normal to the wall, and the origin $z=0$ to be midway between the walls. In the HNC approximation, the grand potential per unit area with respect to its bulk value, $\Omega[\rho]$, is given by [16]

$$\frac{\beta\Omega[\rho]}{A} = \int dz\, dw\, \rho(z,w)\left[\ln\left(\frac{w_T\rho(z,w)}{\rho_B}\right)-1\right] + \beta\int dz\, dw\, \rho(z,w)v(z,w) - \frac{1}{2}\int dz_1 dw_1 dz_2 dw_2 c(z_1,w_1,z_2,w_2,\rho_B) \times\left(\rho(z_1,w_1)-\frac{\rho_B}{w_T}\right)\left(\rho(z_2,w_2)-\frac{\rho_B}{w_T}\right), \quad (1)$$

where $w\equiv(\theta,\varphi)$ denotes the molecular orientation,

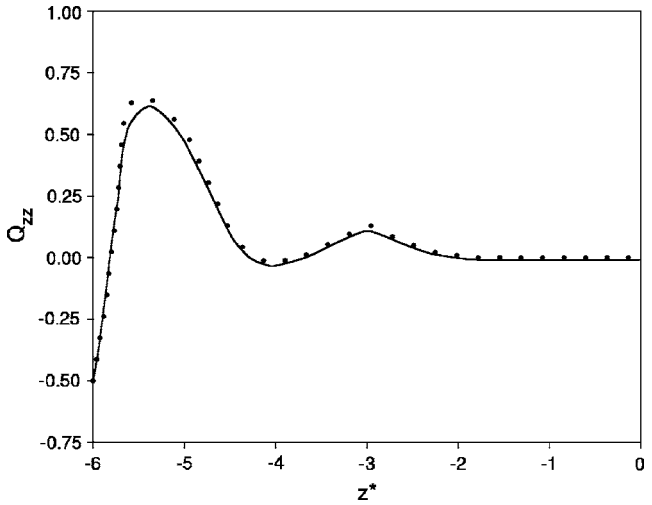

FIG. 2. Order parameter as a function of z^*, using the same parameters as in Fig. 1. The solid curve is our calculation and the dots are from the Monte Carlo simulation [22].

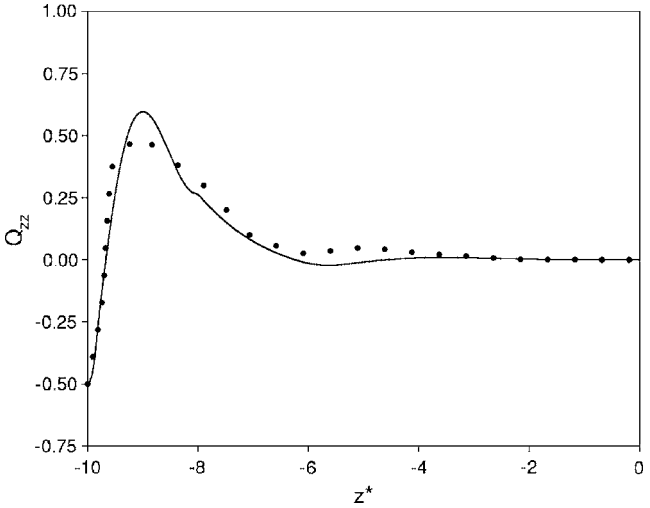

FIG. 4. Order parameter as a function of z^*, using the same parameters as in Fig. 3. The solid curve is our calculation and the dots are from the Monte Carlo simulation [29].

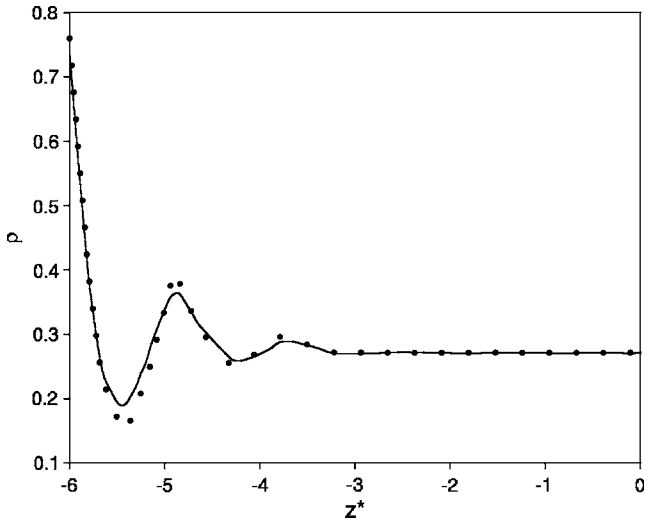

FIG. 5. Number density profiles of molecules as a function of reduced distance from the wall, z^*, for $k=3$, $\rho_B=0.246$, $k_s=2.4$, and $h^*=12$. The solid curve is our calculation and the dots are from the Monte Carlo simulation [22].

$\beta=1/k_BT$, A is the surface area perpendicular to the z axis, ρ_B is the bulk density of the fluid, $v(z,w)$ is the external potential, and $c(z_1,w_1,z_2,w_2;\rho_B)$ is written as

$$c(z_1,w_1,z_2,w_2;\rho_B)=\frac{1}{A}\int dx_1dy_1dx_2dy_2C(\mathbf{r}_1,w_1,\mathbf{r}_2,w_2;\rho_B), \tag{2}$$

where $C(\mathbf{r}_1,w_1,\mathbf{r}_2,w_2;\rho_B)$ is the direct correlation function (DCF) of a homogeneous fluid. In Eq. (1), w_T is the total solid angle available to each molecule. We assume that each molecule can be aligned in $N=2m^2$ different directions, $w_{\alpha\beta}\equiv(\theta_\alpha,\varphi_\beta)$, and choose

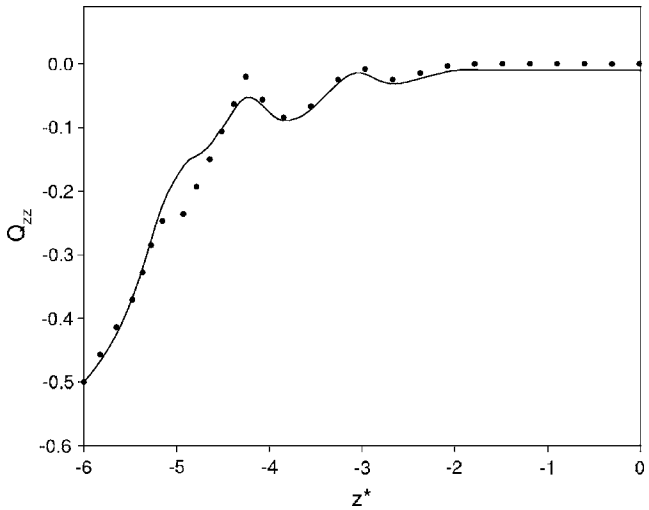

FIG. 6. Order parameter as a function of z^*, using the same parameters as in Fig. 5. The solid curve is our calculation and the dots are from the Monte Carlo simulation [22].

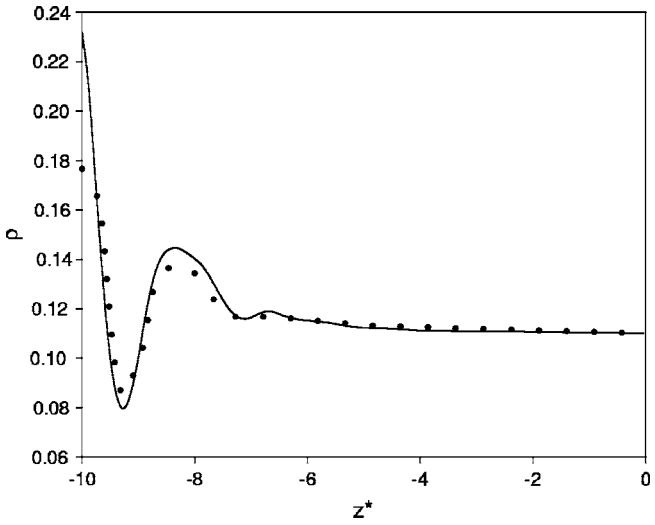

FIG. 7. Number density profiles of molecules as a function of z^* for $k=5$ $k_s=4$, $\rho_B=0.1$, and $h^*=20$. The solid curve is our calculation and the dots are from the Monte Carlo simulation [29].

$$\cos\theta_\alpha=-1+\frac{2\alpha+1}{m},\quad \alpha=0,1,\ldots,m-1 \tag{3}$$

and

$$\varphi_\beta=\beta\frac{\pi}{m},\quad \beta=0,\ldots,2m-1. \tag{4}$$

These allowed directions are uniformly distributed over the surface of a sphere, so equal weighting can be assigned to them. In Eq. (1), the integral of the number density, $\rho(z,w)$, over all orientations, is replaced by a sum of density components, $\rho_{\alpha\beta}(z)$, over allowed orientations $w_{\alpha\beta}$, where

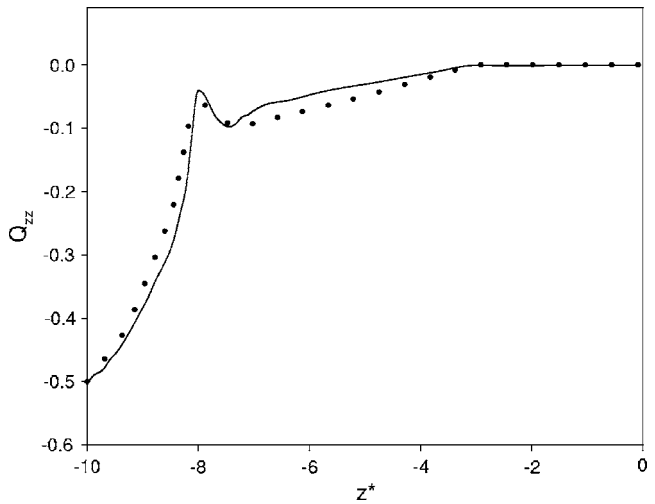

FIG. 8. Order parameter as a function of z^*, using the same parameters as in Fig. 7. The solid curve is our calculation and the dots are from the Monte Carlo simulation [29].

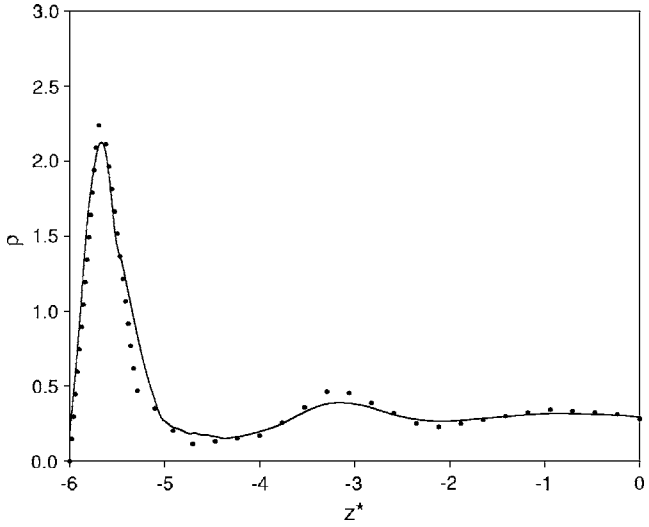

FIG. 9. Number density profiles of molecules as a function of z^* for $k=3$ $k_s=0.6$ $\rho_B=0.325$, and $h^*=12$. The solid curve is our calculation and the dots are from the Monte Carlo simulation [29].

$$\int dw\, \rho(z,w) = \sum_{\alpha\beta} \rho_{\alpha\beta}(z). \tag{5}$$

In a homogeneous fluid we have

$$\sum_{\alpha,\beta} \rho_{\alpha\beta}(z) = N\rho_{\alpha\beta}(z) = \rho_B. \tag{6}$$

The particle-wall interaction has been modeled using a hard needle-wall (HNW) potential, where the particle-surface interaction is represented by a needle, of reduced length k_s, located at the center of of the particle [5,19,22]. More detail is given in Ref. [22]. Thus the HNW potential is defined as

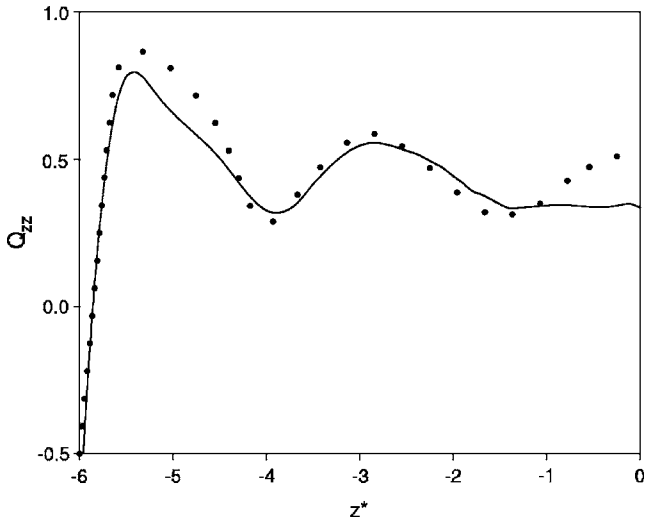

FIG. 10. Order parameter as a function of z^*, using the same parameters as in Fig. 9. The solid curve is our calculation and the dots are from the Monte Carlo simulation [29].

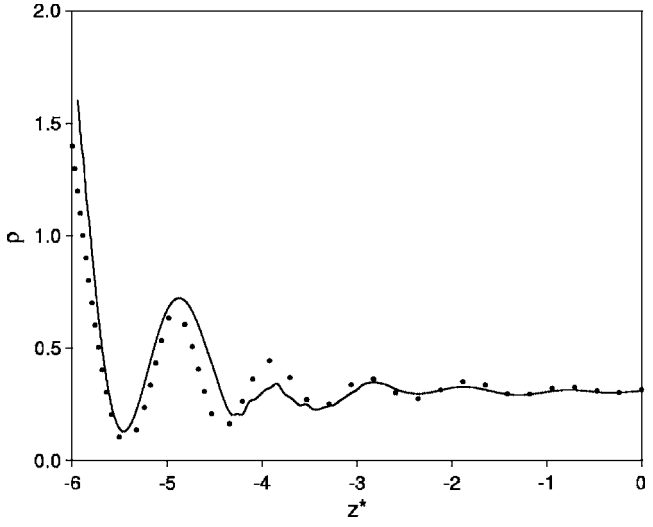

FIG. 11. Number density profiles of molecules as a function of z^* for $k=3$, $k_s=2.4$, $\rho_B=0.325$, and $h^*=12$. The solid curve is our calculation and the dots are from the Monte Carlo simulation [29].

$$v(z,\theta_\alpha) = \begin{cases} 0, & \text{if } h/2 + z \geqslant \sigma_w \text{ and } h/2 - z \geqslant \sigma_w \\ \infty & \text{otherwise,} \end{cases} \tag{7}$$

and

$$\sigma_w = |bk_s \cos\theta_\alpha|, \tag{8}$$

where $2b$, the length of the minor axis of the molecules, is assumed to be the unit length here, h is the separation of the walls, and the coordinates (z,θ_α) refer to the position and orientation of the molecules. Consequently, $\rho_{\alpha\beta}(z)=0$ for $|z|>h_\alpha/2$, where

$$\frac{h_\alpha}{2} = \frac{h}{2} - \sigma_w. \tag{9}$$

Equation (1) is therefore approximated by

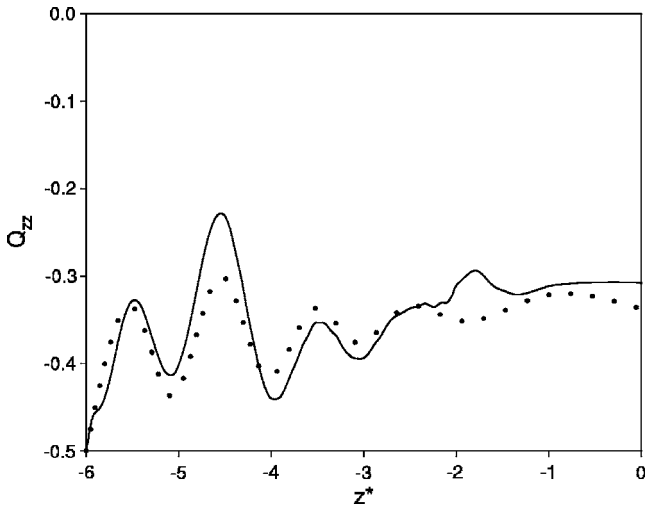

FIG. 12. Order parameter as a function of z^*, using the same parameters as in Fig. 11. The solid curve is our calculation and the dots are from the Monte Carlo simulation [29].

$$\frac{\beta\Omega[\rho_{\alpha\beta}]}{A} = \sum_{\alpha,\beta}\int_{-h_\alpha/2}^{h_\alpha/2} dz\,\rho_{\alpha\beta}\left[\ln\left(\frac{N\rho_{\alpha\beta}(z)}{\rho_B}\right)-1\right] + \beta\sum_{\alpha,\beta}\int_{-h_\alpha/2}^{h_\alpha/2} dz\,\rho_{\alpha\beta}(z)v(z,\theta_\alpha) - \frac{1}{2}\sum_{\alpha,\beta}\sum_{\gamma,\delta}\int_{-h_\alpha/2}^{h_\alpha/2} dz_1\int_{-h_\gamma/2}^{h_\gamma/2} dz_2 c_{\alpha\beta\gamma\delta}(z_1-z_2) \times\left(\rho_{\alpha\beta}(z_1)-\frac{\rho_B}{N}\right)\left(\rho_{\gamma\delta}(z_2)-\frac{\rho_B}{N}\right), \tag{10}$$

where A is the area of the walls and

$$c_{\alpha\beta\gamma\delta}(z_1-z_2) \equiv c(z_1,w_{\alpha\beta},z_2,w_{\gamma\delta};\rho_B). \tag{11}$$

The function $c_{\alpha\beta\gamma\delta}(z_1-z_2)$ depends on the z component of the distance between two molecules.

Minimizing Eq. (10) with respect to the density with no external potential other than the hard needle wall, gives a coupled integral equation:

$$\rho_{\alpha\beta}(z) = \frac{\rho_B}{N}\exp\left[\sum_{\gamma=0}^{m-1}\sum_{\delta=0}^{2m-1}\int dz_1 c_{\alpha\beta\gamma\delta}(z_1-z) \times\left(\rho_{\gamma\delta}(z_1)-\frac{\rho_B}{N}\right)\right]. \tag{12}$$

The symmetry about the z axis implies that for any value of the angle φ_β the density profiles are equal. Thus φ_β can be taken to be zero and we can write

$$\rho_\alpha(z) = \frac{\rho_B}{N}\exp\left[\sum_{\gamma=0}^{m-1}\int dz_1\left(\rho_\gamma(z_1)-\frac{\rho_B}{N}\right)\sum_{\delta=0}^{2m-1} c_{\alpha 0\gamma\delta}(z_1-z)\right]. \tag{13}$$

In this equation, $\rho_\alpha(z)$ is the number density of molecules for any given value of φ and θ_α. From the DCF of the homogeneous HGO fluid, and from the coupled integral equations, Eq. (13), the density profile of confined fluid is calculated, and thereby the surface anchoring can be studied.

III. THE DIRECT CORRELATION FUNCTION OF HGO FLUID

The interaction between two hard ellipsoidal particles by means of the HGO potential is given by

$$U_{12}(\vec{r}_{12},w_1,w_2) = \begin{cases} 0 & \text{if } r_{12} \geqslant \sigma(\hat{r}_{12},w_1,w_2) \\ \infty & \text{if } r_{12} < \sigma(\hat{r}_{12},w_1,w_2), \end{cases} \tag{14}$$

where $w_i=(\theta_i,\varphi_i)$ describes the orientation of the major axis of particle i and $\hat{r}_{12}=\mathbf{r}_{12}/r_{12}$ is a unit vector along the line connecting the centers of the two particles. The range parameter σ, which represents the closest approach distance [21], is given by

$$\sigma(\hat{r}_{12},w_1,w_2) = 2b\left[1-\frac{1}{2}\chi\left\{\frac{(\hat{r}_{12}\cdot\hat{w}_1+\hat{r}_{12}\cdot\hat{w}_2)^2}{1+\chi(\hat{w}_1\cdot\hat{w}_2)} + \frac{(\hat{r}_{12}\cdot\hat{w}_1-\hat{r}_{12}\cdot w_2)^2}{1-\chi(\hat{w}_1\cdot\hat{w}_2)}\right\}\right]^{-1/2}, \tag{15}$$

where

$$\hat{w}_i = (\cos\varphi_i\sin\theta_i,\sin\varphi_i\sin\theta_i,\cos\theta_i) \tag{16}$$

and

$$\chi = \frac{(k^2-1)}{(k^2+1)}. \tag{17}$$

The elongation k is the ratio of the length $2a$ to the breath $2b$ of ellipsoids, $k=2a/2b$. The DCF of a fluid of hard ellipsoids has been calculated by Allen *et al.* [23] using the Monte Carlo simulation method. They compared their results with various theories, and found that the DCF obtained by Marko [24] was closer to their simulation results than the others. Here we use the improved Pynn-Wulf [25,26] expression for the DCF of hard ellipsoids proposed by Marko:

$$C(r_{12},w_1,w_2) = C_{PY}\left(\left[\frac{|\mathbf{r}_2-\mathbf{r}_1|}{\sigma(\hat{r}_{12},w_1,w_2)}\right]\right)[1+\alpha p_2(\hat{w}_1\cdot\hat{w}_2)], \tag{18}$$

where $p_2(t)=(3t^2-1)/2$, $C_{PY}(r)$ is the Percus-Yevick DCF [11] for hard spheres, and $\sigma(\hat{r}_{12},w_1,w_2)$ is the closest approach of HGO particles. We obtain the optimum value of the parameter α by the variational method introduced by Marko. The obtained DCF of the HGO fluid is in agreement with the result obtained by Letz and Latz [27].

IV. RESULTS AND DISCUSSION

We use the HNC density functional theory described in Sec. II to find the density profile and order parameters of a HGO fluid confined between walls using a hard-needle-wall potential, Eq. (7). Barmes and Cleaver [22] have presented a study of the effect of confinement on a system of hard Gaussian ellipsoids interacting with planar substrates through the hard-needle-wall potential using Monte Carlo simulation. They also studied the effects of varying density and particle-substrate interaction, and found an anchoring transition, from planar to homeotropic alignment, at a reduced needle length of $k_s^T \approx 1.4451$, and $k_s^T \approx 3.420$ for elongations $k=3$ and $k=5$, respectively. We compare our results for the cases of homeotropic $k_s < k_s^T$ and planar $k_s > k_s^T$ alignment with the Monte Carlo simulation obtained by Barmes and Cleaver [22]. In our calculation we have used the grand canonical ensemble where in the equilibrium case, the bulk density is related to chemical potential and in our system they are constant [28]. We choose the bulk number density ρ_B to yield to the same mean number density which is defined as

$$\tilde{\rho} = \frac{\int_0^{h^*} dz \rho(z)}{h^*}, \tag{19}$$

or imposed number density $\tilde{\rho}=n/V$, used in the Monte Carlo simulations, which is a canonical ensemble, where n is the number of the particles in the simulation box, V is the volume of the box, and $h^*=h/2b$ is the reduced walls' separation. In our calculations we choose $h^*=12$ for $k=3$ and $h^*=20$ for $k=5$ as it is used in the simulations. In Eq. (19), $\rho(z)=[1/w_T]\int \rho(z,w)dw$ is the angular average number density and hereafter we call it density. We also introduce the orientational order parameter;

$$Q_{zz}(z) = [1/w_T] \int \rho(z,w) P_2(w) dw/\rho(z), \tag{20}$$

which gives the fractional molecules oriented along the z axis and provides information on the surface-induced ordering with respect to the substrate normal. Function $P_2(w)$ is the second Legendre polynomial. We then solve the coupled integral equations (13) for $N=512$, by using an iterative method.

In Fig. 1, for elongation $k=3$, reduced needle length $k_s=0.6$, and bulk density $\rho_B=0.246(\tilde{\rho}=0.28)$, the density profile is plotted as a function of the distance from the center of the slit, $z^*=z/2b$. Also the orientational order parameter $Q_{zz}(z)$ is plotted in Fig. 2. The Monte Carlo simulation results [22] are also plotted for comparison. In Figs. 3 and 4, the density profile and order parameter are plotted and compared, for $k=5$, $k_s=1$, and $\rho_B=0.1(\tilde{\rho}=0.11)$, with the Monte Carlo simulation [29].

As Figs. 1 and 3 show, the density profile $\rho(z)$ rises to a maximum close to the walls, and is an oscillatory function of distance. The main peak is located at a distance $|z^*+h^*/2| \simeq k_s/2$ from the wall and corresponds to the first layer of molecules. These four figures also show that most of the molecules are perpendicular to the walls, because when the density is a maximum, $Q_{zz}(z)$ is positive, and when the density is minimum, very close to the walls, $Q_{zz}(z)$ is negative. These surface-induced changes are associated with a homeotropic arrangement. Positive Q_{zz} means that particles on average are aligned along the z axis or perpendicular to the walls whereas negative Q_{zz} corresponds to the situation when the orientations of particles are close to the xy plane or parallel to the walls [30].

We next consider the effect of increasing the reduced needle length $k_s \geqslant k_s^T$ used in the particle-wall interaction. For $k=3$, $k_s=2.4$, and $\rho_B=0.246(\tilde{\rho}=0.28)$, the density profile and order parameter are plotted in Figs. 5 and 6 respectively. For $k=5$, $k_s=4$, and $\rho_B=0.1(\tilde{\rho}=0.11)$, the density profile and order parameter are plotted in Figs. 7 and 8. As is seen in Figs. 5 and 7, the main peak of the density profile is located at a distance $|z^*+h^*/2| \simeq 0$ from the walls. Since in both Figs. 6 and 8 the order parameter, $Q_{zz}(z)$, is negative near the walls, the particles are arranged in layers with a side by side alignment between one layer and the next. In this case, planar anchoring is occurring.

Now we calculate the density and order parameter profiles of liquid crystal between the walls for the bulk nematic phase. According to the Barmes-Cleaver [22,29] simulation, the isotropic (nematic) coexistance densities are $\rho_I=0.299(\rho_N=0.309)$, hence we do our calculations for $\rho_B>0.31$. In this case we solve the integral equation (13) numerically to obtain the density and order parameter profiles. We chose the bulk density $\rho_B=0.325(\tilde{\rho}=0.34)$ which is in the nematic phase. The calculation should be carefully executed to obtain the required convergence. Therefore, we used the Picard method in our iteration technique, mixing the new results, $\rho_{out}^i(z)$, with the old one $\rho_{in}^i(z)$, as shown below

$$\rho_{in}^{i+1}(z,w) = \alpha \rho_{out}^i(z,w) + (1-\alpha)\rho_{in}^i(z,w,). \tag{21}$$

In addition a suitable choice of the mixing parameter α, is necessary, which was chosen to be $\alpha<0.005$. Here we do the calculations for $k=3$, $\rho_B=0.325(\tilde{\rho}=0.34)$, and $h^*=12$. For $k_s=0.6$ the obtained density and order parameter profiles are compared with the simulations in Figs. 9 and 10, respectively. Later for $k_s=2.4$ these quantities are plotted and compared in Figs. (11) and (12). It is shown in these figures that the obtained density profiles are in agreement with the Monte Carlo simulation whereas the order parameters are fairly in agreement with the simulation except for the region in the middle of the walls. The main reason for this discrepancy in our calculations is due to using the integral equations (13) instead of Eqs. (12). In Eqs. (13) we have assumed an azimuthal symmetry about the z axis to make the numerical calculation possible.

In conclusion, the present calculations showed that the HNC density functional theory can be usefully applied to confined liquid crystals comprising HGO particles with various elongations, and to different lengths of hard needles, representing various particle-substrate interaction through the hard-needle-wall potential, and that it can correctly predict both homeotropic and planar anchoring of molecules at surfaces.

ACKNOWLEDGMENTS

One of us, M. Moradi, would like to thank the research council of Shiraz University. Part of this work was supported by the University of Nottingham.

[1] B. Jerome, Rep. Prog. Phys. **54**, 391 (1991).
[2] J. W. Goodby, Liq. Cryst. **24**, 25 (1998).
[3] T. Geelhaar, Liq. Cryst. **24**, 91 (1998).
[4] P. I. C. Teixeira and T. J. Sluckin, J. Chem. Phys. **97**, 1498 (1992).
[5] D. J. Cleaver and P. I. C. Teixeira, Chem. Phys. Lett. **338**, 1 (2001).
[6] M. P. Allen, Mol. Phys. **96**, 1391 (1999).
[7] P. Pieranski, B. Jerome, and M. Gabay, Mol. Cryst. Liq. Cryst. **179**, 285 (1990).
[8] T. J. Slukin, Physica A **213**, 105 (1995).
[9] H. Lange and F. Schmid, Eur. Phys. J. E **7**, 175 (2002).
[10] H. Lange and F. Schmid, Comput. Phys. Commun. **147**, 276 (2002).
[11] J. P. Hansen and I. R. McDonald, *Theory of Simple Liquids* (Academic, London, 1976).
[12] E. Velesco and L. Mederos, J. Chem. Phys. **109**, 2361 (1998).
[13] E. Velesco, A. M. Somoza, and L. Mederos, J. Chem. Phys. **102**, 8107 (1996).
[14] L. Onsager, Ann. N.Y. Acad. Sci. **51**, 627 (1949).
[15] G. Rickayzen, Mol. Phys. **95**, 393 (1998).
[16] P. Kalpaxis and G. Rickayzen, Mol. Phys. **80**, 391 (1993).
[17] M. Calleja and G. Rickayzen, J. Phys.: Condens. Matter **7**, 8839 (1995).
[18] G. Rickayzen, Mol. Phys. **80**, 1093 (1993).
[19] A. Chrzanowska, P. I. C. Teixeira, H. Ehrentraut, and D. J. Cleaver, J. Phys.: Condens. Matter **13**, 4715 (2001).
[20] B. J. Berne and P. Pechukas, J. Chem. Phys. **64**, 4213 (1972).
[21] E. de Miguel and E. M. del Rio, J. Chem. Phys. **115**, 9072 (2001).
[22] F. Barmes and D. J. Cleaver, Phys. Rev. E **69**, 061705 (2004).
[23] M. P. Allen, C. P. Mason, E. de Miguel, and J. Stelzer, Phys. Rev. E **52**, R25 (1995).
[24] J. F. Marko, Phys. Rev. A **39**, 2050 (1989).
[25] R. Pynn, Solid State Commun. **14**, 29 (1974).
[26] A. Wulf, J. Chem. Phys. **67**, 2254 (1977).
[27] M. Letz and A. Latz, Phys. Rev. E **60**, 5865 (1999).
[28] G. Rickayzen and A. Augousti, Mol. Phys. **52**, 1355 (1984).
[29] F. Barmes, Ph.D. thesis, Sheffield, Hallam University (2003).
[30] A. Poniewierski, Phys. Rev. E **47**, 3396 (1993).